

# Impact Response of FRP Composites Used in Civil Structural Applications <sup>†</sup>

Luis M. Ferreira <sup>1,2\*</sup>, Carlos A.C.P. Coelho <sup>3</sup> and Paulo N.B. Reis <sup>4</sup>

<sup>1</sup> Grupo de Elasticidad y Resistencia de Materiales. Escuela Técnica Superior de Ingeniería. Universidad de Sevilla. Camino Descubrimientos, S/N 41092 Sevilla. Spain

<sup>2</sup> Escuela Politécnica Superior. Universidad de Sevilla. C/ Virgen de África, 7, 41011 Sevilla. Spain

<sup>3</sup> Unidade Departamental de Engenharias. Escola Superior de Tecnologia de Abrantes. Instituto Politécnico de Tomar. Rua 17 de Agosto de 1808 S/N 2200-370 Abrantes. Portugal; cccampos@ipt.pt

<sup>4</sup> University of Coimbra, CEMMPRE, ARISE, Department of Mechanical Engineering, 3030-194 Coimbra, Portugal; paulo.reis@dem.uc.pt

\* Correspondence: lmarques@us.es

<sup>†</sup> The 1<sup>st</sup> International Online Conference on Buildings: Advances in Building Planning, Design Construction, and Operation, Online Conference, 24<sup>th</sup> – 26<sup>th</sup> October 2023.

**Abstract:** This study delves into the effect of repeated low-velocity impacts on the residual tensile strength of composite laminates reinforced with E-glass/epoxy woven fabrics. The specimens underwent a series of low-velocity impacts, each delivering a constant energy of 4 J. Various parameters such as maximum impact load, displacement, contact time, and absorbed energy were examined. The residual tensile strength was subsequently analyzed for each impact and compared to control specimens that experienced no impact. The results highlighted a significant decrease in residual tensile strength after the initial impact, while subsequent impacts exhibited a diminished effect until the puncture of the specimens occurred.

**Keywords:** Low-velocity impacts; Composites; Residual strength; Mechanical testing.

**Citation:** Ferreira, L.M.; Carlos A.C.P. Coelho; Paulo N.B. Reis Impact Response of FRP Composites Used in Civil Structural Applications. **2023**, *5*, x. <https://doi.org/10.3390/xxxxx> Published: 24 October

**Publisher's Note:** MDPI stays neutral with regard to jurisdictional claims in published maps and institutional affiliations.



**Copyright:** © 2023 by the authors. Submitted for possible open access publication under the terms and conditions of the Creative Commons Attribution (CC BY) license (<https://creativecommons.org/licenses/by/4.0/>).

## 1. Introduction

The application of composite materials in the civil engineering sector has been growing due to their advantages, such as: freedom of design, high specific strength and stiffness compared to traditionally used materials, and good chemical resistance to most civil environments. However, published studies mainly address the advantages obtained with these materials, to the detriment of their structural response. An example of this is the impact response, loading mode to which they are very sensitive, because the residual mechanical properties are significantly affected.

In this context, it is possible to find some studies (numerical and experimental) that analyze the influence of several parameters such as energy and geometry of the impactor, stacking sequence [1–5]. On the other hand, in terms of residual strength, they focus essentially on compression after impact (CAI) [6], and few address the tensile loading mode [7]. Therefore, recognizing this gap, this study aims at comprehensively understanding and augmenting the available literature on the post-impact tensile mechanical response of woven glass fibre-reinforced polymer composite structures, also referred to as Tension After Impact (TAI). Understanding how the residual strength of composite materials is affected by impact events will enable architects and engineers to make informed decisions when selecting materials and designing structures that can withstand unforeseen incidents. Ultimately, this work aims to elevate the standards of building construction by integrating the crucial aspect of post-impact tensile strength into the design process, ensuring robustness and resilience in the face of real-world challenges.

## 2. Experimental Procedure

Composite laminate plates were fabricated using a bi-directional E-glass fabric (EC9 68x2) in conjunction with an epoxy resin (SR1500) and a hardener (SD2503). The woven fabric layers were stacked to fabricate 10 ply laminate woven fabric reinforced composites. To ensure optimal impregnation, resin film infusion (RFI) was employed. After this stage, the composite plates were positioned within a vacuum bag for 12 hours at room temperature, employing a maximum pressure of 0.5 mbar. This step served the dual purpose of eliminating any trapped air bubbles and maintaining a consistent fibre volume fraction and uniform thickness. Subsequently, the plates underwent an 8-hour curing process at 60°C.

The specimens were cut to dimensions of 250 mm (length) x 25 mm (width) using a diamond saw. A total of 25 specimens were prepared, with 5 serving as control specimens (0 impacts), and 5 specimens for each impact count (1, 2, 3, and 5). The average thickness of the specimens was  $1.86 \pm 0.048$  mm. It is important to note that aluminium end tabs were bonded to the specimens for the tensile tests, as shown in Figure 1(a). To determine the fibre weight ratio, a burnout test was conducted in accordance with ASTM D3171-15 [8]. The results revealed a fibre weight ratio of 63.9%, which corresponds to a fibre volume fraction of about 47%. Table 1 provides a summary of the experimental tests carried out in this study.

**Table 1.** Summary of the conducted experimental tests.

Number of tested specimens	Number of impacts	Experimental tests
5	0 (control specimen)	Static tensile test
5	1	LVI + TAI
5	2	LVI + TAI
5	3	LVI + TAI
5	5	LVI + TAI

The low-velocity impact (LVI) tests were conducted utilizing the IMATEK-IM10 drop weight testing machine shown in Figure 1(b). A 10 mm diameter impactor with a mass of 2.823 kg was employed. The drop height was defined so that the impact energy was of 4 J. It is important to note that this energy level induced visible damage in a single impact, yet it did not lead to complete puncture of the specimens, thus allowing for a thorough assessment of the post-impact mechanical response. Further details about the drop weight testing machine can be found in [9].

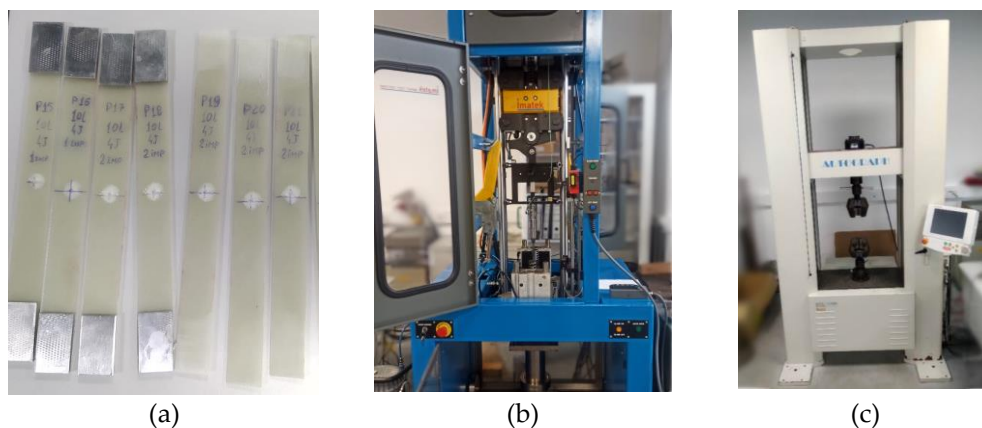


**Figure 1.** (a) Woven fabric composite specimens after being impact, with and without tabs. (b) Drop weight testing machine IMATEK-IM10. (c) Universal testing machine Shimadzu AG-100.

Following each impact, a visual inspection of the specimens was conducted. Leveraging the material's translucency, photos were taken with intense backlighting to facilitate the identification and delineation of the damaged area.

The static tensile strengths of the control specimens (zero impacts) and the impacted specimens were obtained using the universal testing machine Shimadzu AG-100 represented in Figure 1(c), with 3 mm/min displacement rate. All the experimental tests were carried out at standard room temperature.

### 3. Results and Discussion

Representative force-time, force-displacement, and energy-time impact response curves for the  $[0,90]_{10}$  woven fabric composite laminates are shown in Figures 2, 3 and 4 respectively. It can be observed in Figure 1, that the impact force initially rises over time until it reaches a peak value, after which it gradually decreases due to the impactor's rebound until returning to zero. At this instant, the impactor loses contact with the sample.

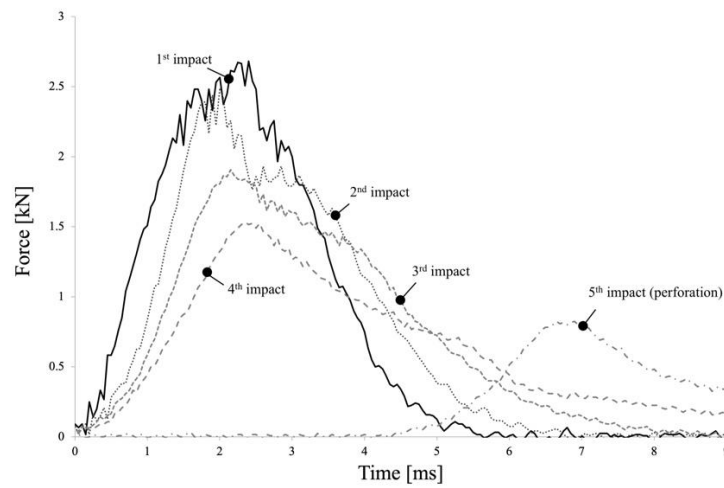


Figure 2. Force-time curves for the repeated low-velocity impacts.

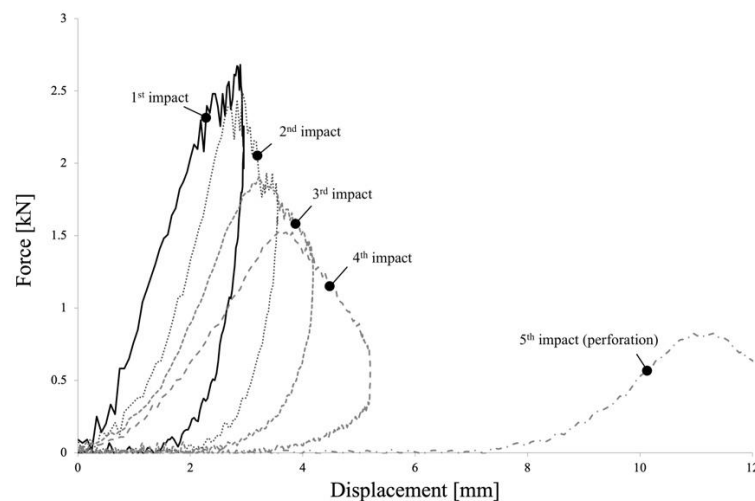


Figure 3. Force-displacement curves for the repeated low-velocity impacts.

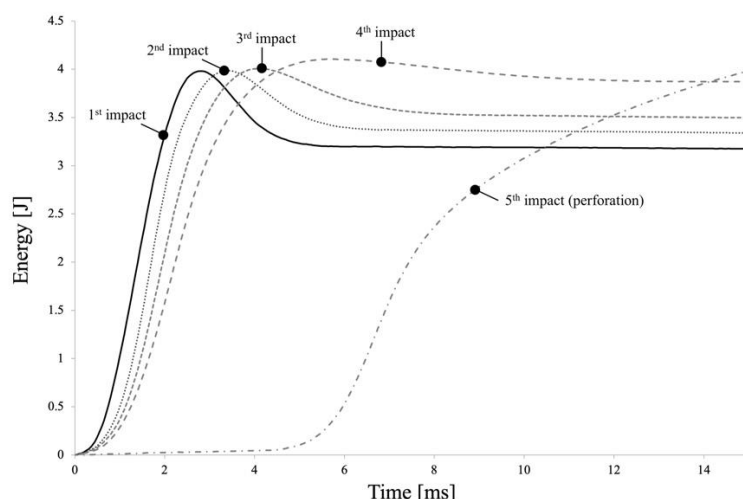
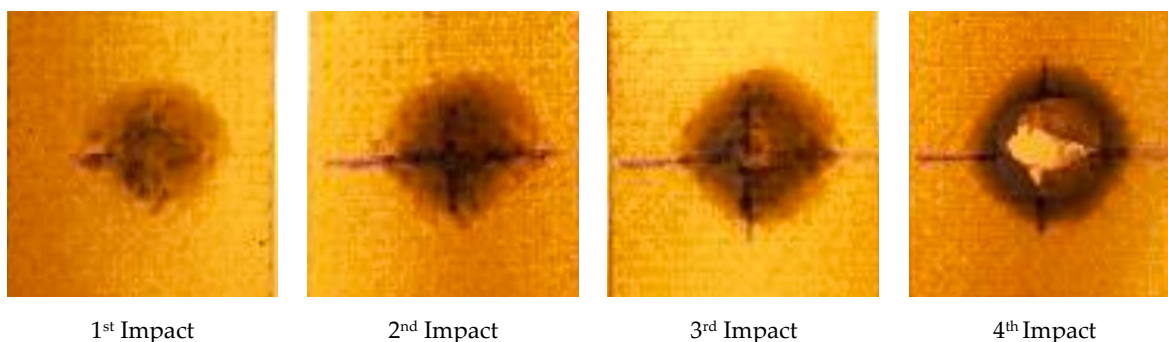


Figure 4. Energy-time curves for the repeated low-velocity impacts.

This consistent profile is observed across all impacts. It is noteworthy that the maximum force diminishes after each impact. For example, in comparison to the first impact, the maximum force decreases by approximately 7.6% at the 2<sup>nd</sup> impact, 30% at the 3<sup>rd</sup> impact, 42.6% at the 4<sup>th</sup> impact, and 68.4% at the 5<sup>th</sup> impact. Examining the maximum displacement depicted in Figure 3, it shows an increase of around 20.7% after the 2<sup>nd</sup> impact, and from that point onwards, it approximately doubles its value with each subsequent impact. It is possible to appreciate in the energy-time curves represented, Figure 4, that the absorbed energy, up until the 4<sup>th</sup> impact, is not sufficiently high to cause puncture of the specimens. The impactor strikes the specimen, rebounds, and does not penetrate fully. However, at the 5<sup>th</sup> impact, full perforation occurs, resulting in the complete absorption of all impact energy. Moreover, it can be observed that the absorbed impact energy steadily increases after each impact. For example, compared to the 1<sup>st</sup> impact, the absorbed energy is 7.9% higher at the 2<sup>nd</sup> impact, and it further increases by 12% and 20.9% at the 3<sup>rd</sup> and 4<sup>th</sup> impacts, respectively. Finally, the contact time also extends with each subsequent impact. For example, the contact time increases by approximately 16% from the 1<sup>st</sup> to the 2<sup>nd</sup> impact, while it rises by about 44.8% and 124.2% at the 3<sup>rd</sup> and 4<sup>th</sup> impacts, respectively.

Figure 5 provides a visual representation of representative damaged areas resulting from impacts 1 to 4. Since the specimens are already completely perforated at the 5<sup>th</sup> impact, their corresponding damaged areas were not included in the analysis. Upon the 1<sup>st</sup> impact, damage in the form of delamination is observed around the impact point, exhibiting a circular shape. This delamination area becomes more pronounced with the 2<sup>nd</sup> impact. While the damaged area seemingly remains unchanged at the 3<sup>rd</sup> impact, the failure of fibres becomes evident, resulting in partial puncture that becomes clearly visible by the 4<sup>th</sup> impact.



1<sup>st</sup> Impact

2<sup>nd</sup> Impact

3<sup>rd</sup> Impact

4<sup>th</sup> Impact

Figure 5. Damage evolution until puncture of the composite specimens.

1  
2

3  
4  
5  
6  
7  
8  
9  
10  
11  
12  
13  
14  
15  
16  
17  
18  
19  
20  
21  
22  
23  
24  
25  
26

To assess the residual tensile strength of the multi-impacted specimens, static tensile tests were conducted. The residual tensile strength, for both the impacted specimens and the control ones, is shown in Figure 6.

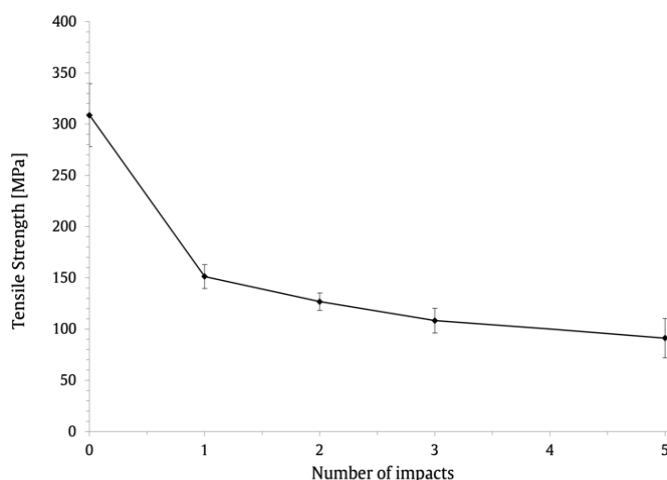


Figure 6. Effect of number of impacts on the residual tensile strength.

The results emphasize the strong influence of the number of impacts on the residual tensile strength, particularly following the 1<sup>st</sup> impact. A clear distinction can be observed between two distinct stages: the initial stage between the control specimens and the 1<sup>st</sup> impact, and the subsequent stage encompassing impacts 2 to 5. It is evident that the tensile strength experiences a substantial decrease from 308.7 N to 151.2 N during the initial stage, corresponding to a reduction of approximately 51%. During the second stage, encompassing impacts 2 to 5, the rate of decrease in tensile strength diminishes to approximately 39.7%. These results indicate that, in static terms, the effect of the introduced damage becomes less pronounced as the number of impacts increases. However, it is important to note that the overall tensile strength continues to be impacted by the cumulative damage inflicted by multiple impacts.

Finally, to gain further insights into the effect of damage on the residual tensile strength, representative static stress-strain curves for both the control and multi-impacted specimens are presented in Figure 7. It can be observed that a substantial loss of stiffness occurs in the multi-impacted specimens, and that as expected, increasing the number impacts leads to a reduction of the specimen’s stiffness.

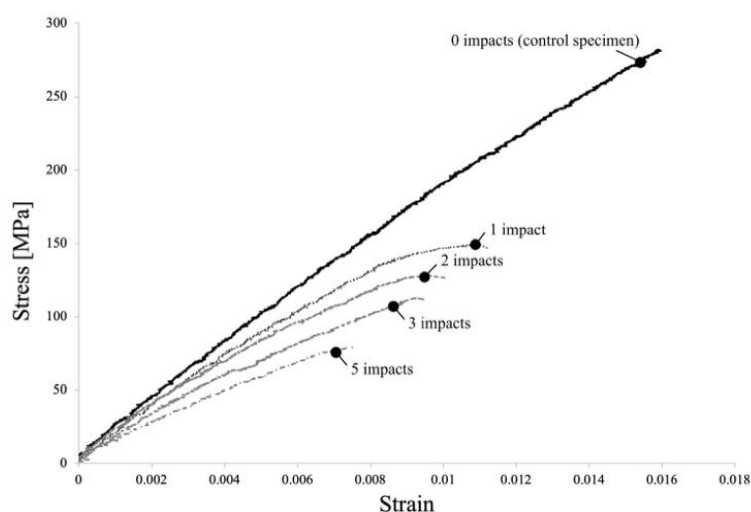


Figure 7. Representative tensile stress-strain curves for the control specimen and multi-impacted specimens.

#### 4. Conclusions

In this experimental study, the effects of repeated low-velocity impacts on the residual tensile strength of woven fabric reinforced composite laminates was investigated. The comprehensive analysis involved evaluating the force and energy histories, as well as various parameters including maximum impact force and displacement, absorbed energy, contact time, static tensile behaviour, and damage evolution.

It was observed that the maximum impact force decreases with the number of impacts, but the reduction is only substantial starting at the 3<sup>rd</sup> impact. The maximum displacement increases about 20.7% after the 2<sup>nd</sup> impact and it approximately doubles its value with each subsequent impact. Additionally, it was seen that the absorbed impact energy steadily increases after each impact and at the 5<sup>th</sup> impact, when full perforation occurs, the impact energy is completely absorbed. Finally, it was found that the contact time also extends with each subsequent impact.

The findings revealed a significant decrease in the residual tensile strength after the 1<sup>st</sup> impact, amounting to a reduction of approximately 51%. This highlights the immediate and substantial impact of the initial damage on the tensile strength of the specimens. Furthermore, the findings indicate that the subsequent impacts, leading up to full perforation, had a relatively diminished effect on the residual tensile strength. From the 2<sup>nd</sup> to the 5<sup>th</sup> impact, it was observed a decrease of approximately 39.7% in the tensile strength. This implies that, in terms of static behaviour, the effectiveness of the damage inflicted by subsequent impacts becomes less pronounced.

The progression of damage throughout the multiple impacts was also analysed. The observed decrease in tensile strength corresponds to the evolving damage mechanisms and the interaction between the impacted areas.

These results underscore the importance of considering the cumulative effects of multiple low-velocity impacts on the residual tensile strength of composite laminates. The findings have significant implications for building design and construction, emphasizing the need to account for potential damage and degradation in structures subjected to repeated impacts.

**Author Contributions:** Conceptualization, C.A.C.P. Coelho and L.M. Ferreira; methodology, C.A.C.P. Coelho and L.M. Ferreira; formal analysis, C.A.C.P. Coelho, L.M. Ferreira and P.N.B. Reis; investigation, C.A.C.P. Coelho, L.M. Ferreira and P.N.B. Reis; resources L.M. Ferreira and C.A.C.P. Coelho; writing—original draft preparation, L.M. Ferreira, C.A.C.P. Coelho and P.N.B. Reis; writing—review and editing, L.M. Ferreira, C.A.C.P. Coelho and P.N.B. Reis. All authors have read and agreed to the published version of the manuscript.

**Funding:** This research received no external funding.

**Data Availability Statement:** The data presented in this study are available on request from the corresponding author.

**Acknowledgments:** This research was sponsored by national funds through FCT-Fundação para a Ciência e a Tecnologia, under the projects UIDB/00285/2020 and LA/P/0112/2020.

**Conflicts of Interest:** The authors declare no conflict of interest.

#### References

1. L. Ferreira; C. Coelho; P. Reis Impact Response of Semi-Cylindrical Composite Laminate Shells Under Repeated Low-Velocity Impacts. In Proceedings of the 2022 Advances in Science and Engineering Technology International Conferences (ASET); February 21 2022; pp. 1–5.
2. Reis, P.N.B.; Sousa, P.; Ferreira, L.M.; Coelho, C.A.C.P. Multi-Impact Response of Semicylindrical Composite Laminated Shells with Different Thicknesses. *Compos. Struct.* **2023**, *310*, 116771, doi:10.1016/j.compstruct.2023.116771.
3. Ferreira, L.M.; Coelho, C.A.C.P.; Reis, P.N.B. Numerical Simulations of the Low-Velocity Impact Response of Semicylindrical Woven Composite Shells. *Materials* **2023**, *16*, doi:10.3390/ma16093442.

4. Ferreira, L.M.; Coelho, C.A.C.P.; Reis, P.N.B. Effect of Cohesive Properties on Low-Velocity Impact Simulations of Woven Composite Shells. *Appl. Sci.* **2023**, *13*, 6948, doi:10.3390/app13126948. 1
5. Ferreira, L.M.; Coelho, C.A.C.P.; Reis, P.N.B. Numerical Predictions of Intralaminar and Interlaminar Damage in Thin Composite Shells Subjected to Impact Loads. *Thin-Walled Struct.* **2023**, *192*, 111148, doi:10.1016/j.tws.2023.111148. 2
6. Davies, G.; Olsson, R. Impact on Composite Structures. *Aeronaut. J.* **2004**, *108*, 541–563. 3
7. Ferreira, L.M.; Coelho, C.A.C.P.; Reis, P.N.B. Residual Tensile Strength of Multi-Impacted Woven Glass Fibre-Reinforced Polymer Composites. In Proceedings of the Experimental Mechanics in Engineering and Biomechanics; INEGI / FEUP (Faculty of Engineering of University of Porto): Porto, Portugal, July 2023; pp. 269–270. 4
8. D30 Committee *Test Methods for Constituent Content of Composite Materials*; ASTM International; 5
9. Ferreira, L.M.; Aranda, M.T.; Muñoz-Reja, M.; Coelho, C.; Távara, L. Ageing Effect on the Low-Velocity Impact Response of 3D Printed Continuous Fibre Reinforced Composites. *Compos. Part B Eng.* **2023**, 111031, doi:10.1016/j.compositesb.2023.111031. 6

**Disclaimer/**

12

13